doi:10.1038/nature13794

Helium and lead isotopes reveal the geochemical geometry of the Samoan plume

M. G. Jackson[1], S. R. Hart[2], J. G. Konter[3], M. D. Kurz[4], J. Blusztajn[2] & K. A. Farley[5]

Hotspot lavas erupted at ocean islands exhibit tremendous isotopic variability, indicating that there are numerous mantle components[1,2] hosted in upwelling mantle plumes that generate volcanism at hotspots like Hawaii and Samoa[3]. However, it is not known how the surface expression of the various geochemical components observed in hotspot volcanoes relates to their spatial distribution within the plume[4–10]. Here we present a relationship between He and Pb isotopes in Samoan lavas that places severe constraints on the distribution of geochemical species within the plume. The Pb-isotopic compositions of the Samoan lavas reveal several distinct geochemical groups, each corresponding to a different geographic lineament of volcanoes. Each group has a signature associated with one of four mantle endmembers with low $^3He/^4He$: EMII (enriched mantle 2), EMI (enriched mantle 1), HIMU (high $\mu = {}^{238}U/{}^{204}Pb$) and DM (depleted mantle). Critically, these four geochemical groups trend towards a common region of Pb-isotopic space with high $^3He/^4He$. This observation is consistent with several low-$^3He/^4He$ components in the plume mixing with a common high-$^3He/^4He$ component, but not mixing much with each other. The mixing relationships inferred from the new He and Pb isotopic data provide the clearest picture yet of the geochemical geometry of a mantle plume, and are best explained by a high-$^3He/^4He$ plume matrix that hosts, and mixes with, several distinct low-$^3He/^4He$ components.

Lavas erupted at oceanic hotspots—thought to sample melts from buoyantly upwelling mantle plumes[3]—are isotopically heterogeneous and provide definitive evidence that the Earth's mantle is compositionally diverse and hosts several distinct geochemical groups[1,2]. Radiogenic isotopic studies of ocean island basalts erupted at hotspots identify a multitude of mantle compositions that are often broadly grouped into four endmembers with different isotopic taxonomies: EMII, EMI, HIMU and DM. A fifth component, characterized by high $^3He/^4He$ ratios, is also identified in ocean island basalts[11], and has been variously called undegassed mantle[12], FOZO (focus zone[13]), PHEM (primitive helium mantle[14]), or C (common[15]). Unfortunately, the spatial distribution of these mantle components within upwelling mantle plumes is difficult to infer using geochemical studies of surficially erupted basalts.

Recent efforts to examine the spatial distribution of mantle plume geochemical heterogeneities have focused on the geographic distribution of isotopic compositions along the surface volcanic traces of hotspot tracks. These studies have yielded significant progress relating the distribution of isotopic compositions in surface lavas to the spatial distribution of isotopic components within an upwelling mantle plume. A well known geographic separation of isotopic compositions occurs at the Hawaiian hotspot, where two parallel volcanic lineaments—Loa and Kea—exhibit compositions that can be isotopically resolved[4–6,16]. The isotopic and geographic separation of the Loa and Kea volcanic lineaments is suggested to reflect the spatial separation of the mantle components within the plume that give rise to the two isotopically distinct volcanic lineaments, which is possibly related to the compositional structure of the deepest mantle[5,6]. Similar observations of geographical and geochemical separations of parallel volcanic lineaments have been made at other hotspots[6–10,17]. These observations suggest that the geochemical structure of many mantle plumes vary spatially in a systematic manner.

This paper focuses on the geochemical variability along the parallel volcanic lineaments of the age-progressive[18] Samoan hotspot and the geochemical structure of the underlying upwelling mantle plume. We present 36 new Pb-isotopic analyses together with new Sr, Nd and He isotopic measurements (Supplementary Tables 1–3) on a suite of lavas from the Samoan hotspot (Fig. 1 and Extended Data Fig. 1). In $^{206}Pb/^{204}Pb$–$^{208}Pb/^{204}Pb$ isotopic space, four isotopic groups emerge from the data set (Fig. 2), and the four groups converge on a common region, roughly forming an X shape. Three of the four isotopic groups are defined by shield-stage lavas from each of three volcanic lineaments that tend to form separate groups in isotopic space: the islands and seamounts of the Vai volcanic lineament (dark blue shading and symbols); the Malu volcanic lineament (pink); and subaerial lavas from the Upo volcanic lineament (yellow) (Fig. 1). Rejuvenated-stage lavas are encountered only on the islands of Savai'i, Upolu and Tutuila (which define the Upo volcanic lineament), are younger than the shield-stage lavas on each island, and form a fourth isotopic group (turquoise).

There are exceptions to this correspondence between geochemistry and geography (Methods). For example, the submarine lavas from the western region of the hotspot (dredged near Savai'i and Upolu islands) overlap with the isotopic compositions found in the Vai and Malu-volcanic lineaments further to the east and include ultra-enriched lavas[18,19] unlike those found in any of the younger and more easterly volcanism (Fig. 2); this enriched material includes an additional isotopic component in the Samoan plume. However, there are insufficient submarine samples from the western Samoan region to define their isotopic taxonomy or geographic extent, or whether the western Samoan submarine samples define separate geographic trends, and we exclude these submarine lavas from our treatment below (see Methods); this approach is similar to that taken in Hawaii, where the geochemical separation of the Loa and Kea volcanic lineaments breaks down in the western region of the Hawaiian chain, and it is common to exclude some or all of the western islands when defining the Loa and Kea lineaments[4]. In this paper we examine Samoan rejuvenated lavas, Vai- and Malu-lineament lavas, and the subaerial shield lavas from the Upo-lineament, which form four geochemical groups. However, submarine western Samoan lavas are shown in the figures for clarity.

The four geochemical groups identified in Samoan rejuvenated lavas, Vai- and Malu-lineament lavas, and the subaerial shield lavas from the Upo lineament are clearly resolved as separate clusters in multiple isotopic spaces (Fig. 2; Methods). Lavas from the four groups exhibit geochemical characteristics that are associated with the four canonical mantle endmembers, as follows. The Malu group has EM2 characteristics, the Vai group has HIMU characteristics (though the signature is dilute), the Upo group has geochemically depleted characteristics (not unlike

[1]Department of Earth Science, University of California Santa Barbara, Santa Barbara, California 93106-9630, USA. [2]Department of Geology and Geophysics, Woods Hole Oceanographic Institution, Woods Hole, Massachusetts 02543, USA. [3]Department of Geology and Geophysics, School of Earth and Ocean Sciences and Technology (SOEST), University of Hawaii, Manoa, Honolulu, Hawaii 96822, USA. [4]Department of Marine Chemistry, Woods Hole Oceanographic Institution, Woods Hole, Massachusetts 02543, USA. [5]Division of Geological and Planetary Sciences, California Institute of Technology, Pasadena, California 91125, USA.

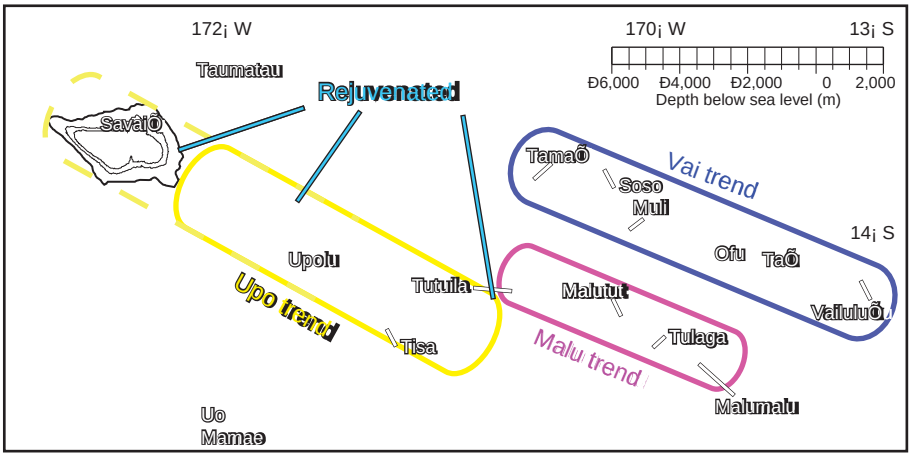

Figure 1| Map of the Samoan hotspot showing the division of the hotspot into three parallel volcanic lineaments. The volcanic lineaments define three geochemical groups, and the colours of the data symbols in the isotopic plots (see Figs 1 and 2) indicate the volcanic lineament from which a sample was taken. Rejuvenated lavas (turquoise shaded areas) overlie shield-stage lavas on Tutuila and Upolu, but rejuvenated volcanism on Savai•i is extensive and all earlier stages have been completely covered.[21] However, ref. 28 infers that, like Upolu and Tutuila, shield-stage volcanism similar to the subaerial Upo-lineament lavas (called the •Fagaloa series•) underlies the extensive rejuvenated volcanism on Savai•i. The map is modified after ref. 21. Alexa seamount is located about 1,200 km west of Sava•i.[29,30]

Hawaiian Mauna Kea lavas; Fig. 2), and rejuvenated lavas have EM1 characteristics (see Methods).

These four endmember groups appear to converge in a region of isotopic space characterized by lavas with the highest $^3He/^4He$ values, and the ellipse describing the highest $^3He/^4He$ lavas (20…33.8 Ra, ratio to atmosphere)[14,17,20] in Fig. 2 serves as a common component region for the four Samoan geochemical groups (see Methods). In two- and three-dimensional Pb-isotopic space, the four Pb-isotopic data groups overlap with the common component region at the 99% confidence level (Fig. 2 and refer to Methods). Additionally, in Pb-isotopic space $^3He/^4He$ ratios decrease monotonically away from the common region towards the extremes of the four data groups located furthest from the common region. We quantify this relationship by calculating the distance from the common component in three-dimensional Pb-isotopic space, and the distance parameter is called $D^{206-207-208}Pb$ (Methods). $^3He/^4He$ is highest in the common component region (low $D^{206-207-208}Pb$ values) and decreases away from the common component (high $D^{206-207-208}Pb$) (Fig. 3).

The unique isotopic topology identified in Samoan lavas places important constraints on the distribution and mixing relationships of the various components in the Samoan plume. The data are consistent with the low-$^3He/^4He$ components (that is, 8 Ra) in the plume mixing with a high-$^3He/^4He$ common component, and this mixing hypothesis is supported by the relationship between $^3He/^4He$ and $D^{206-207-208}Pb$ (Fig. 3) and by the convergence of the four 99% confidence intervals that enclose all possible mixing trends for each group (Fig. 2). The four low-$^3He/^4He$ components do not appear to mix efficiently with each other, otherwise the four Pb-isotopic groups would be obscured. However, some mixing among the low-$^3He/^4He$ components has occurred, and this might explain

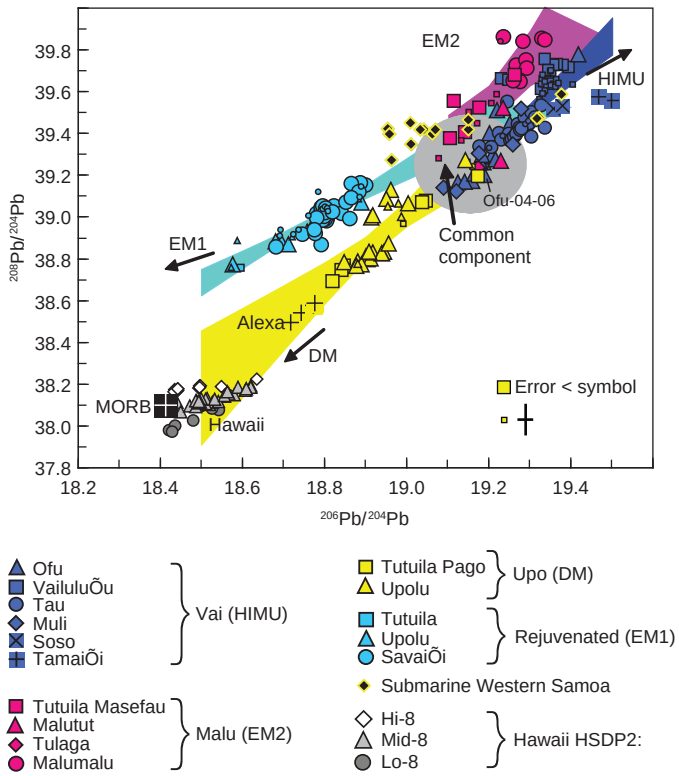

Figure 2| Pb-isotopic plot showing the isotopic separation of the volcanic lineaments in Samoa and the convergence of the four geochemical groups on the high-$^3He/^4He$ component region. The colours for each data group are based on the geographic lineament where the samples were taken. Samples for which Pb-isotopic ratios were measured by high-precision techniques (Pb-spiked samples run by thermal ionization mass spectrometer (TIMS) and samples run using Tl-addition by multi-collector inductively coupled plasma mass spectrometer (MC-ICP-MS)) are shown as large symbols (where estimated external uncertainties are smaller than the symbols). Unspiked Pb-isotopic TIMS data are shown as small symbols (where estimated 2s external uncertainties are better than 0.019, 0.023 and 0.076 for $^{206}Pb/^{204}Pb$, $^{207}Pb/^{204}Pb$ and $^{208}Pb/^{204}Pb$, respectively; see Methods); example 2s external uncertainties for unspiked Pb-isotopic TIMS data are shown. Subaerial Upo-lineament lavas trend towards a depleted component not unlike that found in mid-ocean ridge basalt (MORB) or Hawaiian lavas from the HSDP-2 (Hawaiian Scientific Drilling Program-II) drill core. Alexa[29,30] is a volcano in the western Samoan region that anchors the DM isotopic group in the Samoan suite (Methods). The submarine lavas from the western region of the hotspot, dredged off the coast of Savai•i and from the Tisa seamount, are excluded from the statistical treatment; although the lavas from the submarine portion of the western Samoan islands are shown with the same symbol (yellow diamonds), this does not imply that they are related by a common process or part of the same volcanic lineament. Vai-lineament lavas host a dilute HIMU component[17], Malu-lineament lavas host an EM2 component[17], and rejuvenated lavas sample an EM1 component.[21,31] The high-$^3He/^4He$ common component region (grey ellipse) defines the 2s variance around the average in the Pb-isotopic compositions for samples with $^3He/^4He$ > 20 Ra; the coloured shading represents 99% confidence intervals around the best-fit lines through each data group (see Methods). See Supplementary Table 4 for a compilation of the Samoan data shown.

2. Hofmann, A. in *The Mantle and Core* (ed. Carlson, R. W.) Vol. 2 *Treatise in Geochemistry* 61–101 (Elsevier, 2003).
3. Morgan, W. J. Convection plumes in the lower mantle. *Nature* **230,** 42–43 (1971).
4. Abouchami, W. *et al.* Lead isotopes reveal bilateral asymmetry and vertical continuity in the Hawaiian mantle plume. *Nature* **434,** 851–856 (2005).
5. Weis, D., Garcia, M. O., Rhodes, J. M., Jellinek, M. & Scoates, J. S. Role of the deep mantle in generating the compositional asymmetry of the Hawaiian mantle plume. *Nature Geosci.* **4,** 831–838 (2011).
6. Huang, S., Hall, P. S. & Jackson, M. G. Geochemical zoning of volcanic chains associated with Pacific hotspots. *Nature Geosci.* **4,** 874–878 (2011).
7. Payne, J. A., Jackson, M. G. & Hall, P. S. Parallel volcano trends and geochemical asymmetry of the Society Islands hotspot track. *Geology* **41,** 19–22 (2013).
8. Rohde, J. *et al.* 70 Ma chemical zonation of the Tristan-Gough hotspot track. *Geology* **41,** 335–338 (2013).
9. Harpp, K. S., Hall, P. S. & Jackson, M. G. in *The Galápagos: A National Laboratory for the Earth Sciences* (eds Mittelstaedt, E., Graham, D., d'Ozouville, N. & Harpp, K.) 27–40 (AGU, in the press).
10. Chauvel, C. *et al.* The size of plume heterogeneities constrained by Marquesas isotopic stripes. *Geochem. Geophys. Geosyst.* **13,** Q07005 (2012).
11. Stracke, A., Hofmann, A. W. & Hart, S. R. FOZO, HIMU and the rest of the mantle zoo. *Geochem. Geophys. Geosyst.* **6,** http://dx.doi.org/10.1029/2004GC000824 (2004).
12. Kurz, M. D., Jenkins, W. J. & Hart, S. R. Helium isotopic systematics of oceanic islands and mantle heterogeneity. *Nature* **297,** 43–47 (1982).
13. Hart, S. R., Hauri, E. H., Oschmann, L. A. & Whitehead, J. A. Mantle plumes and entrainment: isotopic evidence. *Science* **256,** 517–520 (1992).
14. Farley, K. A., Natland, J. H. & Craig, H. Binary mixing of enriched and undegassed (primitive?) mantle components (He, Sr, Nd, Pb) in Samoan lavas. *Earth Planet. Sci. Lett.* **111,** 183–199 (1992).
15. Hanan, B. B. & Graham, D. W. Lead and helium isotope evidence from oceanic basalts for a common deep source of mantle plumes. *Science* **272,** 991–995 (1996).
16. Tatsumoto, M. Isotopic composition of lead in oceanic basalt and its implication to mantle evolution. *Earth Planet. Sci. Lett.* **38,** 63–87 (1978).
17. Workman, R. K. *et al.* Recycled metasomatized lithosphere as the origin of the Enriched Mantle II (EM2) endmember: evidence from the Samoan volcanic chain. *Geochem. Geophys. Geosyst.* **5,** http://dx.doi.org/10.1029/2003GC000623 (2004).
18. Koppers, A. A. P. *et al.* Samoa reinstated as a primary hotspot trail. *Geology* **36,** 435–438 (2008).
19. Jackson, M. G. *et al.* The return of subducted continental crust in Samoan lavas. *Nature* **448,** 684–687 (2007b).
20. Jackson, M. G., Kurz, M. D., Hart, S. R. & Workman, R. K. New Samoan lavas from Ofu Island reveal a hemispherically heterogeneous high $^{3}He/^{4}He$ mantle. *Earth Planet. Sci. Lett.* **264,** 360–374 (2007a).
21. Konter, J. G. & Jackson, M. G. Large volumes of rejuvenated volcanism in Samoa: Evidence supporting a tectonic influence on late-stage volcanism. *Geochem. Geophys. Geosyst.* **13** (2012).
22. Farnetani, C. G., Hofmann, A. W. & Class, C. How double volcanic chains sample geochemical anomalies from the lowermost mantle. *Earth Planet. Sci. Lett.* **359/360,** 240–247 (2012).
23. Harpp, K. S. *et al.* in *The Galápagos: A National Laboratory for the Earth Sciences* (eds Mittelstaedt, E., Graham, D., d'Ozouville, N. & Harpp, K.) (AGU, in the press).
24. Bryce, J. G., DePaolo, D. J. & Lassiter, J. C. Geochemical structure of the Hawaiian plume: Sr, Nd, and Os isotopes in the 2.8 km HSDP-2 section of Mauna Kea volcano. *Geochem. Geophys. Geosyst.* **6,** Q09G18 (2005).
25. Coltice, N., Moreira, M., Hernlund, J. & Labrosse, S. Crystallization of a basal magma ocean recorded by helium and neon. *Earth Planet. Sci. Lett.* **308,** 193–199 (2011).
26. Mukhopadhyay, S. Early differentiation and volatile accretion recorded in deep-mantle neon and xenon. *Nature* **486,** 101–104 (2012).
27. Li, M., McNamara, A. K. & Garnero, E. J. Chemical complexity of hotspots caused by cycling oceanic crust through mantle reservoirs. *Nature Geosci.* http://dx.doi.org/10.1038/ngeo2120 (2014).
28. Natland, J. H. The progression of volcanism in the Samoan linear volcanic chain. *Am. J. Sci.* **280A,** 709–735 (1980).
29. Hart, S. R. *et al.* Genesis of the Western Samoa (WESAM) seamount province: age, geochemical fingerprint and tectonics. *Earth Planet. Sci. Lett.* **227,** 37–56 (2004).
30. Eisele, J., Abouchami, W., Galer, S. J. G. & Hofmann, A. W. The 320 kyr Pb isotope evolution of Mauna Kea lavas recorded in the HSDP-2 drill core. *Geochem. Geophys. Geosyst.* **4,** http://dx.doi.org/10.1029/2002GC000339 (2003).

Supplementary Information is available in the online version of the paper.

Acknowledgements We thank J. Natland, P. Hall and M. Regelous for discussions, and R. Carlson for access to analytical facilities. Comments from B. Hanan and K. Harpp improved the manuscript. M.G.J. acknowledges grants from the NSF that funded this research: OCE-1061134, OCE-1153894, EAR-1348082 and EAR-1145202.

Author Contributions M.G.J. conceived of the project, performed most of the Sr, Nd and Pb isotopic analyses, and wrote the paper. S.R.H. provided analytical access and insights into the nature of the Samoan mantle. J.G.K. performed statistical modelling, improved figures, and added discussion about the volcanic stages during the evolution of a Samoan volcano. M.D.K. performed helium isotopic measurements, K.A.F. performed helium isotopic measurements and some Sr and Nd isotopic measurements, and J.B. helped with sample preparation and made several Sr and Pb isotopic measurements. All authors contributed intellectually to the manuscript.

Author Information Reprints and permissions information is available at www.nature.com/reprints. The authors declare no competing financial interests. Readers are welcome to comment on the online version of the paper. Correspondence and requests for materials should be addressed to M.G.J. (jackson@geol.ucsb.edu).

METHODS

New Sr, Nd, Pb and He isotopic measurements. The new Pb-isotopic analyses were performed at the DTM (Department of Terrestrial Magnetism) and WHOI (Woods Hole Oceanographic Institution). Pb chemistry at DTM employs a double column pass and follows the method outlined in ref. 31. Pb chemistry at WHOI consists of a single column pass and follows the HBr-HNO_3 procedure of ref. 32 and ref. 33.

As described in Supplementary Table 1, Pb isotopic compositions for a subset of the Samoan lavas were measured on the VG-P54 MC-ICP-MS at DTM in February 2009. Refer to ref. 34 for methods of Pb-isotopic measurement. Thallium was added as an internal isotopic standard to correct for instrumental mass fractionation. All measurements were made during a single day-long analytical session, during which time eight separate runs of the NIST 981 standard were made, and the reproducibility of the eight measurements was 840 parts per million (p.p.m.), 820 p.p.m. and 800 p.p.m. for the $^{206}Pb/^{204}Pb$, $^{207}Pb/^{204}Pb$ and $^{208}Pb/^{204}Pb$ ratios (2σ, standard deviation of the mean). The Pb-isotopic data on basaltic samples run during this analytical session were normalized to the average value determined by the 981 analyses that bracket the basaltic analyses over the analytical session. The data were normalized to the NIST 981 values reported by ref. 35: $^{206}Pb/^{204}Pb = 16.9356$, $^{207}Pb/^{204}Pb = 15.4891$ and $^{208}Pb/^{204}Pb = 36.7006$.

The remaining Pb-isotopic measurements reported in Supplementary Table 1 were made on the Neptune multicollector ICP-MS at WHOI over six separate analytical sessions from November 2003 to October 2008. Note that many of the samples measured for Pb isotopes at WHOI were previously measured by lower-precision TIMS methods (that is, unspiked analyses), and we report new, higher-precision analyses here. Again, a Tl internal standard was used to correct for instrumental mass fractionation. The long-term external reproducibility on NIST 981 standard runs at WHOI is <120 p.p.m. for the $^{206}Pb/^{204}Pb$, $^{207}Pb/^{204}Pb$ and $^{208}Pb/^{204}Pb$ ratios[29,36]. Basaltic sample runs were normalized to the average NIST 981 value measured in a given analytical session using NIST 981 values reported by ref. 35.

Supplementary Table 2 includes new $^{87}Sr/^{86}Sr$ and $^{143}Nd/^{144}Nd$ isotopic measurements. Analyses made at WHOI follow chemical separation techniques outlined in ref. 29; Sr and Nd isotopic measurements were made on the Neptune multicollector ICP-MS at WHOI, and standard normalization and long-term external precision are described in ref. 29. The Sr and Nd isotopic analyses made at the Scripps Institution of Oceanography follow analytical techniques outlined in ref. 14.

Supplementary Table 3 includes new helium isotopic measurements, which were measured at WHOI and at the Scripps Institution of Oceanography. Measurements made at WHOI follow the methods outlined in ref. 37. All data were obtained by crushing olivines or glasses in vacuum, except for one sample, which is a measurement of gas released by fusion following a crushing experiment. In-run precision is reported in the Supplementary Table 3. Measurements made at the Scripps Institution of Oceanography follow the methods outlined in ref. 14, where uncertainty in $^3He/^4He$ ratios is estimated to be ± 0.5 Ra.

Calculating distance in three-dimensional Pb-isotopic space. The expression for distance in Pb multi-isotopic space, here called $D^{206/207/208Pb}$, is given by the following relationship: $D^{206/207/208Pb} = [((^{206}Pb/^{204}Pb_S - {}^{206}Pb/^{204}Pb_R)/X)^2 + ((^{207}Pb/^{204}Pb_S - {}^{207}Pb/^{204}Pb_R)/Y)^2 + ((^{208}Pb/^{204}Pb_S - {}^{208}Pb/^{204}Pb_R)/Z)^2]^{0.5}$, where the subscript R indicates the isotopic composition of the reference sample, the subscript S is the isotopic composition of any Samoan lava sample, and X, Y and Z represent the absolute difference between the maximum and minimum values measured in Samoan hotspot lavas (including rejuvenated lavas and all lavas from the Vai, Malu and Upo lineaments) for $^{206}Pb/^{204}Pb$ ($X = 19.4993 - 18.5720 = 0.9273$), $^{207}Pb/^{204}Pb$ ($Y = 15.6510 - 15.5538 = 0.0972$) and $^{208}Pb/^{204}Pb$ ($Z = 39.8620 - 38.6929 = 1.1691$), respectively. The reference isotopic composition is chosen to be the highest-$^3He/^4He$ lava from Samoa (Ofu-04-06)[20], which plots near the region of convergence of the four isotopic groups.

The expression for distance ($D^{206/207/208Pb}$) in Pb-isotopic space is based on the Pythagorean theorem, where the differences between each Pb-isotopic ratio and the common component are squared, these squared differences are then summed, and the square root of the sum is taken. The expression for distance in Pb-isotopic space (that is, $D^{206/207/208Pb}$) also accounts for the fact that different Pb-isotopic ratios exhibit dramatically different variability. To do this, the difference in the Pb-isotopic ratio between two data points is divided by the total range measured in Samoan lavas. For example, the total range in $^{206}Pb/^{204}Pb$ in Samoan lavas is 0.9273, which is the difference between the highest measured $^{206}Pb/^{204}Pb$ ratio (19.4993) and the lowest ratio (18.5720). Thus, the $^{206}Pb/^{204}Pb$ ratio exhibits 5.0% variability in Samoan lavas. This is important because, in Samoan lavas, $^{208}Pb/^{204}Pb$ varies from 39.8620 to 38.6929 in Samoa, which represents ~3.0% variability, while $^{207}Pb/^{204}Pb$ exhibits only 0.6% variability (15.6510 to 15.5538 in Samoan lavas). If the distance equation did not normalize the isotopic difference between data points by the total range in the isotopic ratio of interest, then the distances calculated would be dominated by the $^{206}Pb/^{204}Pb$ and $^{208}Pb/^{204}Pb$ variability, and $^{207}Pb/^{204}Pb$ (which has limited variability in Samoa and in the ocean-island-basalt mantle in general) would contribute very little to the overall distance calculated.

We emphasize that the different isotopic groups converge on a common region rather than a point in Pb-isotopic space. No single sample in the existing Samoan data set, including Ofu-04-06, is ideally suited as a point of convergence for all the geochemical groups in Samoa. However, given the limited available data set on high-$^3He/^4He$ Samoan lavas, and given the observation that Ofu-04-06 plots near the region of convergence of the different isotopic groups, we choose the isotopic composition of this lava as a reference isotopic composition in the $D^{206/207/208Pb}$ equation because it has the highest $^3He/^4He$.

Statistical test for the convergence of the four Pb-isotopic groups. The relationship between $^3He/^4He$ and distance from the common component region in Pb-isotopic space—where $^3He/^4He$ decreases with increasing distance (higher $D^{206/207/208Pb}$ values) from the common component region—is consistent with a model in which the four low-$^3He/^4He$ components in the Samoan plume mix with a common high-$^3He/^4He$ component. To evaluate whether the four different isotopic groups—represented by lavas from the Malu, Vai and subaerial-Upo lineaments and rejuvenated lavas (Extended Data Fig. 1)—converge on the high-$^3He/^4He$ common component region in Pb-isotopic space, we first define the high-$^3He/^4He$ common component region to be comprised of all Samoan lavas with $^3He/^4He > 20$ Ra. Since many samples measured for Pb isotopes were not suitable for $^3He/^4He$ measurements, this allows us to compensate for potential under-sampling of the high-$^3He/^4He$ common component and to define uncertainty in the composition of the common component. We model the compositional range of the common component region with the mean and the variance of the Pb-isotope data (and Nd-isotopic data) for samples with $^3He/^4He > 20$ Ra (see Fig. 2 and Extended Data Figs 2 and 3). This results in an ellipsoid centred on the mean value and with major axes defined by the 2σ variations in the heavy radiogenic isotopic compositions. Subsequently, we test whether the four data groups indeed converge on this ellipsoidal common component region, taking advantage of the linearity of mixing relationships in Pb-isotopic space. To model the possible orientations of mixing lines for each group, we use best-fit trends through each group and their related confidence intervals. We computed Working–Hotelling confidence intervals at the 99% confidence level to be as inclusive as possible in visualizing possible mixing lines for each group (we tested 95% confidence as well, and the conclusions are the same). In three-dimensional Pb-isotopic space, the 99% confidence intervals (they appear as 'tubes' in three-dimensional isotopic space; Fig. 2 and Extended Data Figs 2 and 3) around each of the best-fit trend lines overlap with the ellipsoid that encompasses the common component region that is defined by the highest-$^3He/^4He$ lavas. This observation shows that, for each data group, there exists a family of mixing lines (within error of the best-fit line) that statistically overlaps with our common component region. This isotopic overlap also maps to two-dimensional Pb-isotopic spaces (see Fig. 2 and Extended Data Fig. 3), although the three-dimensional case shows that only a subset of possibilities in individual two-dimensional plots is actually possible. In summary, all four of the best-fit trend lines through the four different isotopic groups statistically overlap with the common component region in Pb-isotopic space.

However, we note that submarine lavas from western Samoan (that is, lavas dredged off the coast of Sava'i and Upolu) are excluded from this statistical test. Available data from these lavas do suggest that they follow the relationship between $^3He/^4He$ and distance from the common component region in Pb-isotopic space (Fig. 2), which is consistent with mixing with the common component region. However, the limited sampling of the submarine portion of the western Samoan region makes it difficult to assign the few available samples to geographic groups: For example, only Savai'i (four dredges: ALIA114, ALIA115, ALIA116 and ALIA128) and the Tisa seamount (one dredge; ALIA113) have samples of the deep submarine portions of the western Samoan region, and several of the dredges are distal to the Upo volcanic lineament. Thus, the vast submarine region in western Samoa, which spans around 200 km (from Savai'i to Tisa), is represented by only five submarine dredges, of which several were distal to Savai'i and Upolu, which do not clearly belong to the Upo-lineament (indeed, the distance between the northernmost and southernmost dredges in the western Samoa region is >130 km, which is more than twice the distance that separates the Vai and Malu volcanic lineaments). Our statistical approach requires that the Samoan data are grouped along geographic trends, and we test whether these geographically defined data groups converge on the high-$^3He/^4He$ component region in isotopic space. With such poor sampling along the submarine portion of the western Samoan islands, and the improbability that these dredges sample the same geographic lineament, it is not yet possible to evaluate geographic groups in the isotopic data sets in the submarine portion of the western Samoan region.

Geographic separation of the isotopic components in Samoa. The geographic-isotopic groups (the Vai, Malu and Upo volcanic lineaments and rejuvenated lavas) are resolved in multiple isotopic spaces (Fig. 2, Extended Data Figs 2 and 3). Below,

we describe the seamounts and islands that comprise the four geographic groups that are resolved in isotopic space:

(1) The Vai volcanic lineament is comprised of the islands of Ofu and Ta'u, and Vailulu'u, Soso, Tamai'i and Muli seamounts. In isotopic space, including $^{206}Pb/^{204}Pb$ versus $^{208}Pb/^{204}Pb$, $^{206}Pb/^{204}Pb$ versus $^{207}Pb/^{204}Pb$ and $^{206}Pb/^{204}Pb$ versus $^{143}Nd/^{144}Nd$, some of the Vailulu'u lavas trend slightly outside of the data group formed by other Vai-lineament volcanoes. These anomalous lavas trend in the direction of Malu-lineament lavas in isotopic space, indicating that Vailulu'u samples components similar to that found in the mantle sources of both the Vai and Malu volcanic lineaments, but that lavas from the Vai-lineament rarely sample the component hosted along the Malu volcanic lineament. Two Vailulu'u samples from the same dredge—AVON3-73-1 and AVON-3-73-12—plot squarely in the field defined by Malu-lineament lavas, and show that, like the Hawaiian Loa and Kea volcanic lineaments[4,5], the isotopic separation of the Malu and Vai volcanic lineaments is not perfect. Another lava from the Vai volcanic lineament, Ta'u sample T44, plots closer in isotopic space to lavas that comprise the Malu volcanic lineament. Ta'u sample T14, which exhibits highly unradiogenic Pb and anomalous Pb concentrations relative to other Ta'u lavas[17], may be contaminated and is not shown here.

(2) The Malu volcanic lineament is geographically displaced to the south of the Vai volcanic lineament and is comprised of the Malumalu, Malutut and Tulaga seamounts and the Masefau shield lavas of northeast Tutuila. We find that three Malu-lineament lavas from dredges 108 (DR108) and 109 (DR109) from the ALIA cruise[18,19,38,39] have Vai-lineament-like geochemistry, again showing that the geochemical distinction between the two parallel volcanic ridges is not perfectly resolved in isotopic space.

The Malu volcanic lineament joins seamlessly with the northeast region of the island of Tutuila. Tutuila lavas with geochemistry similar to Malu-lineament lavas, referred to as Masefau shield lavas[14], outcrop only along the north coast of the northeastern region of the island along the Afono, Maefau and Sailele bays (J. Natland, personal communication, 2013). Masefau lavas have not been encountered anywhere else on Tutuila, with the possible exception of sample 91-TP-252, which was collected on the southern coast of the northeast portion of the island (however, this sample is a cobble, so its true provenance is unknown). Less geochemically enriched Tutuila lavas, referred to as Pago shield lavas[14,40], outcrop on the rest of the island. Using radiometric age data from ref. 41, lavas identified geochemically as Pago shield lavas in the western region of the island are generally younger than lavas identified as Masefau shield lavas on the eastern side of the island (see ref. 41 and references therein). Indeed, the Masefau shield sequences are cross-cut by dikes with Pago shield geochemical signatures[14]. Work pairing geochemistry with age data is relatively scarce in Samoa, and further work is needed to evaluate the temporal relationship between the Masefau and Pago shield series. However, from existing data, we argue that Tutuila is divided between two volcanic series, and that the younger Pago shield series overlies much of the older Masefau series, much like the Hawaiian Mauna Loa series overlies the Mauna Kea series in the HSDP2 drill core[42] (we note that these two volcanoes, Mauna Kea and Mauna Loa, sample the separate volcanic lineaments along the Hawaiian hotspot, just as the Pago and Masefau shield sample two separate volcanic lineaments in Samoa). We further argue that the two volcanic series on Tutuila anchor the Upo and Malu volcanic lineaments, both geochemically and geographically. The Malu volcanic lineament joins with the northeastern region of Tutuila where the isotopically related Masefau lavas are encountered, and we argue that Tutuila Masefau lavas anchor the westernmost portion of the Malu lineament (and the Tutuila Pago lavas anchor the easternmost limb of the Upo volcanic lineament; see below).

(3) In the Upo lineament, Pago shield lavas from Tutuila are isotopically similar to subaerial Upolu shield lavas (subaerial Upo-lineament lavas from Upolu have previously been referred to as Fagaloa shield lavas)[40,43], and they outcrop on the western and southern portions of Tutuila (and as dikes cross-cutting the Masefau shield lavas in northeast Tutuila). We argue that the Pago shield lavas mark the easternmost extent of the Upo volcanic lineament, while Tutuila Masefau lavas define the westernmost extent of the Malu volcanic lineament. Thus, Tutuila Island acts as a nexus between the Upo lineament (Pago shield series on southern Tutuila) and the Malu lineament (Masefau shield series on northern Tutuila). In contrast to all other volcanic structures in Samoa, which strike along a direction parallel to absolute plate motion (WNW to ESE), the island of Tutuila is oriented obliquely to plate motion (WSW to ENE)[41]. Thus, the Malu lineament 'steps off' to the northeast, away from the Upo lineament, and Tutuila effectively bridges these two volcanic lineaments.

Shield lavas from Upolu have similar isotopic compositions to Pago shield lavas on Tutuila (Fig. 2, Extended Data Fig. 3), and the Upo volcanic lineament is comprised of lavas from at least two islands. Fagaloa series lavas that define the subaerial Upo lineament also may exist on Savai'i, but if they do, they have been completely covered with young rejuvenated lavas[28].

The volcanic stage suggested for two subaerial Upolu lavas may require new designations, based on their geochemical characteristics. Upolu samples U30L and U10S (see ref. 17) were tentatively classified in the field as rejuvenated-stage lavas on the basis of a geological map from ref. 43. Later isotopic analyses[17] showed that these two samples plot in the field of shield lavas (M. Regelous, personal communication, 2013), and we argue that these two samples belong to the shield stage. We note that Pb-isotopic data reported on Tutuila lavas from the Pago shield (and Upolu lavas) by ref. 44 are severely contaminated and are excluded from the present study[45].

(4) Rejuvenated lavas from the Samoan islands of Savai'i, Upolu and Tutuila have variable extents of rejuvenated lava cover, from only minor rejuvenated volcanism cover on Tutuila to near-complete cover of the shield stage by rejuvenated lavas on Savai'i[21]. In radiogenic isotopic spaces, the rejuvenated lavas form a separate field that is resolved from shield-stage lavas, and the rejuvenated lavas from each island are isotopically similar (Fig. 2, Extended Data Fig. 3). The origin of Samoan rejuvenated lavas—which are volumetrically extensive—is not well understood, but is thought to relate at least partially to tectonically enhanced melting caused by tectonic stresses in the region generated by the nearby Tonga trench[17,21,28,29,40,46].

Geochemical identity of the five mantle components in the Samoan plume. The identity of the four low-$^3He/^4He$ mantle species in the Vai and Malu lineaments, the subaerial Upo lineament and in rejuvenated lavas can be determined by examining their geochemical characteristics. Below, we argue that the four low-$^3He/^4He$ components in the Samoan plume sample the canonical mantle endmembers—EM1, EM2, HIMU and DM—in variably diluted forms. A fifth component, which is characterized by having high $^3He/^4He$, has geochemical signatures that give clues to its origin:

(1) In the Malu lineament, the lavas have geochemical signatures associated with the EM2 mantle endmember, including negative Ti (and Nb, not shown) anomalies (Extended Data Fig. 4), and very high $^{87}Sr/^{86}Sr$ (refs 17 and 19). The earliest shield-stage lavas on Savai'i, dredged on the deep submarine flanks of Savai'i (4.8 to 5.3 million years ago)[18], have isotopic and trace element signatures of an even more extreme EM2 component (with $^{87}Sr/^{86}Sr$ up to 0.7216)[19] that complements the EM2 signature that characterizes Malu lineament volcanics[14,17,47,48]. The EM2 component in Samoa is best modelled by recycling subducted, continentally derived sediment into the Samoan mantle[19,47–49].

(2) In the Vai lineament, lavas have geochemical signatures that are similar to the HIMU mantle endmember (albeit in greatly diluted form). Vai-lineament lavas have the highest (U + Th)/Pb (Extended Data Fig. 5) and the most radiogenic $^{206}Pb/^{204}Pb$ (Fig. 2, Extended Data Fig. 3) in the Samoan suite. High (Th + U)/Pb is a characteristic of HIMU lavas[50]. Clearly, Vai-lineament lavas do not exhibit the highly radiogenic Pb-isotopic compositions evident in HIMU endmember locations like Mangaia and Tubuai (for example, ref. 51), but we argue that Vai-lineament lavas host a dilute HIMU component that is not sampled in pure endmember form in Samoa, at least in lavas studied to date. The most extreme HIMU components in the mantle have been linked to ancient recycled oceanic crust (see, for example, refs 51–54).

(3) In the Upo lineament, subaerial lavas trend towards a depleted mantle composition in various isotopic spaces (Fig. 2, Extended Data Figs 3 and 4), and are characterized by the highest $^{143}Nd/^{144}Nd$ in the Samoan suite. Supporting this hypothesis, $^{143}Nd/^{144}Nd$ increases along the subaerial Upo-lineament group moving away from the high-$^3He/^4He$ common component region (as $D^{206/207/208}Pb$ increases) in the direction of MORB and Hawaiian lavas from the HSDP-2 drill core (Fig. 2, Extended Data Fig. 4). By comparison, the other three data groups exhibit relatively constant or even decreasing $^{143}Nd/^{144}Nd$ with increasing distance from the high-$^3He/^4He$ common component region. (Curiously, $^{143}Nd/^{144}Nd$ exhibits the least amount of variability in the high-$^3He/^4He$ common component region—where $D^{206/207/208}Pb$ is near zero, which indicates that the common component region has relatively homogeneous isotopic characteristics.) Thus, subaerial lavas from the Upo-lineament group appear to sample a depleted mantle composition, a hypothesis that is supported by the observation that average MORB[55] and Hawaii Kea lavas (which exhibit geochemically depleted $^{143}Nd/^{144}Nd$) anchor the data trends for Upolu shield and Tutuila Pago lavas in all isotopic spaces[17]. The western Samoan seamount Alexa[29] anchors the most extreme terminus of the Samoan DM isotopic group sampled by subaerial Upo-lineament lavas; data from this seamount are shown in all relevant isotopic spaces and the data plot near the field for Hawaiian Kea lavas. Therefore, the geochemical component sampled by Upo-lineament lavas is not unlike the depleted plume component sampled by Hawaiian Kea lavas, and may be inherent to the Samoan plume, but we cannot exclude a depleted upper mantle source (like that which sources MORB) as the endmember sampled by Upo-lineament lavas.

(4) In the rejuvenated lavas from Samoa there is a mild EM1 component, and this is supported by positive Ba-anomalies (high Ba/Th in Supplementary Fig. 4) in Samoan rejuvenated lavas[17,29,38], a geochemical characteristic shared with EM1 endmember lavas from Pitcairn[29]. Relative to Samoan shield lavas, Samoan rejuvenated lavas exhibit elevated $^{208}Pb/^{204}Pb$ at a given $^{206}Pb/^{204}Pb$, a characteristic that is also shared with EM1-like lavas globally.

(5) The variably diluted mantle endmembers identified in Samoan lavas—EM2, EM1, HIMU and DM—are known to have relatively low $^3He/^4He$ values[17,19,56–59]. These low-$^3He/^4He$ components anchor the four isotopic groups in the region of isotopic space furthest from the high-$^3He/^4He$ common component region. However, lavas with relatively high to very high $^3He/^4He$ are found on several islands and seamounts (up to 33.4 Ra on Ofu, 18.0 Ra on Ta'u, 25.8 Ra on Tutuila, 19.3 Ra on Upolu, 15.9 Ra on Malumalu, 15.3 Ra on Muli and 18.6 Ra on Savai'i), and these lavas tend to plot near the high-$^3He/^4He$ common component region (Fig. 3; Extended Data Fig. 6). High-$^3He/^4He$ lavas in Samoa have high Ti/Ti* (defined in ref. 19) values[60,61] (in contrast to the low Ti/Ti* observed in the Samoan EM2 endmember; Extended Data Fig. 4). Consistent with this observation, Ti/Ti* is highest near the high-$^3He/^4He$ common component region; moving away from the centre of the common component region (from high to low $D^{206/207/208}Pb$ values), Ti/Ti* decreases in the direction of the four low-$^3He/^4He$ endmembers (Extended Data Fig. 4). This relationship between Ti/Ti* and $^3He/^4He$ is highlighted by the elevated Ti/Ti* observed in high $^3He/^4He$ lavas globally[60].

Samoan lavas with high $^3He/^4He$ are melts of a mantle component with a controversial origin, and these lavas cluster in the common component region in isotopic space (Extended Data Fig. 6). Reference 14 argued that the high-$^3He/^4He$ Samoan component represents primitive, undegassed mantle, and called this component PHEM (primitive helium mantle). However, higher $^3He/^4He$ ratios (up to 33.8 Ra) identified in Samoan lavas have $^{143}Nd/^{144}Nd$ that are geochemically depleted relative to primitive, chondritic material, and Pb-isotopic compositions that are far from the geochron[20]. Nonetheless, high-$^3He/^4He$ Samoan lavas have lower (geochemically more enriched) $^{143}Nd/^{144}Nd$ than lavas with high $^3He/^4He$ from other hotspots[20], and it was suggested that relatively young (about ten million years old) sediments rapidly cycled from the Tonga trench might account for this Nd-isotopic shift[62,63]. However, the Pb-isotopic compositions in Samoan lavas preclude the existence of a young sediment component in the Samoan mantle[19], and sediments from the Tonga trench in particular are a poor fit for Samoan lavas in Pb-isotopic space (see figure 3 in ref. 20). The origin of the enriched geochemical signatures in Samoan high-$^3He/^4He$ lavas is not known, but ref. 20 suggested the involvement of a DUPAL signature—a globe-encircling band of isotopic enrichment observed in Southern Hemisphere hotspot lavas[64]—in the Samoan high-$^3He/^4He$ mantle that shifts the $^{143}Nd/^{144}Nd$ to lower values than observed in Northern Hemisphere high-$^3He/^4He$ hotspot lavas. The origin of the geochemically enriched DUPAL signature is not known, but might relate to ancient (about 1.8 billion years old) subducted material[64]. Thus the unique heavy radiogenic isotopic signature of the Samoan high-$^3He/^4He$ plume component may result from the incorporation of ancient subducted material into the high-$^3He/^4He$ mantle.

31. Carlson, R. W., Czamanske, G., Fedorenko, V. & Ilupin, I. A comparison of Siberian meimechites and kimberlites: implications for the source of high-Mg alkalic magmas and flood basalts. *Geochem. Geophys. Geosyst.* **7,** Q11014 (2006).
32. Galer, S. J. H. *Chemical and Isotopic Studies of Crust–Mantle Differentiation and the Generation of Mantle Heterogeneity*. PhD thesis, Univ. Cambridge (1986).
33. Abouchami, W., Galer, S. J. G. & Koschinsky, A. Pb and Nd isotopes in NE Atlantic Fe–Mn crusts: proxies for trace metal paleosources and paleocean circulation. *Geochim. Cosmochim. Acta* **63,** 1489–1505 (1999).
34. Petrone, C. M., Francalanci, L., Carlson, R. W., Ferrari, L. & Conticelli, S. Unusual coexistence of subduction-related and intraplate-type magmatism: Sr, Nd and Pb isotope and trace element data from the magmatism of the San Pedro-Ceboruco graben (Nayarit, Mexico). *Chem. Geol.* **193,** 1–24 (2003).
35. Todt, W. Cliff, R. A., Hanser, A. & Hofmann, A.W. in *Earth Processes: Reading the Isotopic Code* (eds Basu, A. & Hart, S. R.) *Geophys. Monogr.* **95,** 429–437 (1996).
36. Hart, S. R. *et al.* The Pb isotope pedigree of Western Samoan volcanics: new insights from high-precision analysis by NEPTUNE ICP/MS. *Eos* **83,** F20 (2002).
37. Kurz, M. D., Curtice, J., Lott, D. E., III & Solow, A. Rapid helium isotopic variability in Mauna Kea shield lavas from the Hawaiian Scientific Drilling Project. *Geochem. Geophys. Geosyst.* **5,** Q04G14 (2004).
38. Jackson, M. G. *et al.* The Samoan hotspot track on a ''hotspot highway'': Implications for mantle plumes and a deep Samoan mantle source. *Geochem. Geophys. Geosyst.* **11,** http://dx.doi.org/10.1029/2010GC003232 (2010).
39. Koppers, A. A. P. *et al.* Age systematics of two young en echelon Samoan volcanic trails. *Geochem. Geophys. Geosyst.* **12,** Q07025 (2011).
40. Natland, J. H. & Turner, D. L. in *Geological Investigations of the Northern Melanesian Borderland* (ed. Brocker, T. M.) *Earth Science Series* Vol. 3, 139–172 (Circum-Pacific Council for Energy and Mineral Resources, 1985).
41. Mcdougall, I. Age and evolution of the volcanos of Tutuila, American Samoa. *Pac. Sci.* **39,** 311–320 (1985).
42. Stolper, E. M. & DePaolo, D. M. Introduction to special section: Hawaii Scientific Drilling Project. *J. Geophys. Res.* **101,** 11593–11598 (1996).
43. Kear, D. & Wood, B. L. *The Geology and Hydrology of Western Samoa* New Zealand Geological Survey Bulletin 63 (1959).
44. Palacz, Z. A. & Saunders, A. D. Coupled trace element and isotope enrichment in the Cook-Austral-Samoa islands, southwest Pacific. *Earth Planet. Sci. Lett.* **79,** 270–280 (1986).
45. McDonough, W. & Chauvel, C. Sample contamination explains the Pb isotopic composition of some Rurutu island and Sasha seamount basalts. *Earth Planet. Sci. Lett.* **105,** 397–404 (1991).
46. Hawkins, J. W. & Natland, J. H. Nephelinites and basanites of the Samoan linear volcanic chain: their possible tectonic significance. *Earth Planet. Sci. Lett.* **24,** 427–439 (1975).
47. White, W. M. & Hofmann, A. W. Sr and Nd isotope geochemistry of oceanic basalts and mantle evolution. *Nature* **296,** 821–825 (1982).
48. Wright, E. & White, W. M. The origin of Samoa: new evidence from Sr, Nd, and Pb isotopes. *Earth Planet. Sci. Lett.* **81,** 151–162 (1986).
49. Workman, R. K., Eiler, J. M., Hart, S. R. & Jackson, M. G. Oxygen isotopes in Samoan lavas: confirmation of continent recycling. *Geology* **36,** 551–554 (2008).
50. Hanyu, T. *et al.* Geochemical characteristics and origin of the HIMU reservoir: a possible mantle plume source in the lower mantle. *Geochem. Geophys. Geosyst.* **12,** Q0AC09 (2011).
51. Hauri, E. H. & Hart, S. R. Re-Os isotope systematics of HIMU and EMII oceanic island basalts from the south Pacific ocean. *Earth Planet. Sci. Lett.* **114,** 353–371 (1993).
52. Hauri, E. H. & Hart, S. R. Rhenium abundances and systematics in oceanic basalts. *Chem. Geol.* **139,** 185–205 (1997).
53. Hofmann, A. W. & White, W. M. Mantle plumes from ancient oceanic crust. *Earth Planet. Sci. Lett.* **57,** 421–436 (1982).
54. Cabral, R. A. *et al.* Anomalous sulphur isotopes in plume lavas reveal deep mantle storage of Archaean crust. *Nature* **496,** 490–493 (2013).
55. Gale, A., Dalton, C. A., Langmuir, C. H., Su, Y. & Schilling, J.-G. The mean composition of ocean ridge basalts. *Geochem. Geophys. Geosyst.* **14,** 489–518 (2013).
56. Graham, D. W. *et al.* Helium isotope geochemistry of mid-ocean ridge basalts from the South Atlantic. *Earth Planet. Sci. Lett.* **110,** 133–147 (1992).
57. Parai, R., Mukhopadhyay, S. & Lassiter, J. C. New constraints on the HIMU mantle from neon and helium isotopic compositions of basalts from the Cook–Austral Islands. *Earth Planet. Sci. Lett.* **277,** 253–261 (2009).
58. Hanyu, T. & Kaneoka, I. The uniform and low $^3He/^4He$ ratios of HIMU basalts as evidence for their origin as recycled materials. *Nature* **390,** 273–276 (1997).
59. Honda, M. & Woodhead, J. D. A primordial solar-neon enriched component in the source of EM-I-type ocean island basalts from the Pitcairn Seamounts, Polynesia. *Earth Planet. Sci. Lett.* **236,** 597–612 (2005).
60. Jackson, M. G. *et al.* Globally elevated titanium, tantalum, and niobium (TITAN) in ocean island basalts with high $^3He/^4He$. *Geochem. Geophys. Geosyst.* **9,** http://dx.doi.org/10.1029/2007GC001876 (2008).
61. Hart, S. R. & Jackson, M. Ta'u and Ofu/Olosega volcanoes: the ''Twin Sisters'' of Samoa, their P, T, X melting regime, and global implications. *Geochem. Geophys. Geosyst.* http://dx.doi.org/10.1002/2013GC005221 (2014).
62. Farley, K. A. Rapid cycling of subducted sediments into the Samoan mantle plume. *Geology* **23,** 531–534 (1995).
63. Class, C. & Goldstein, S. L. Evolution of helium isotopes in the Earth's mantle. *Nature* **436,** 1107–1112 (2005).
64. Hart, S. R. A large-scale isotope anomaly in the Southern Hemisphere mantle. *Nature* **309,** 753–757 (1984).
65. Sims, K. W. W. *et al.* ^{238}U-^{230}Th-^{226}Ra-^{210}Po, ^{232}Th-^{228}Ra, and ^{235}U-^{231}Pa constraints on the ages and petrogenesis of Vailulu'u and Malumalu lavas, Samoa. *Geochem. Geophys. Geosyst.* **9,** Q04003 (2008).
66. Hart, S. R. *et al.* Vailulu'u undersea volcano: the new Samoa. *Geochem. Geophys. Geosyst.* **1,** http://dx.doi.org/10.1029/2000GC000108 (2000).
67. Anderson, T. The volcano of Matavanu in Savaii. *Q. J. Geol. Soc. Lond.* **66,** 621–639 (1910).
68. Matsuda, J. I., Notsu, K., Okano, J., Yaskawa, K. & Chungue, L. Geochemical implications from Sr isotopes and K-Ar age determinations for the Cook-Austral Islands chain. *Tectonophysics* **104,** 145–154 (1984).
69. McDougall, I. Age of volcanism and its migration in the Samoa Islands. *Geol. Mag.* **147,** 705–717 (2010).

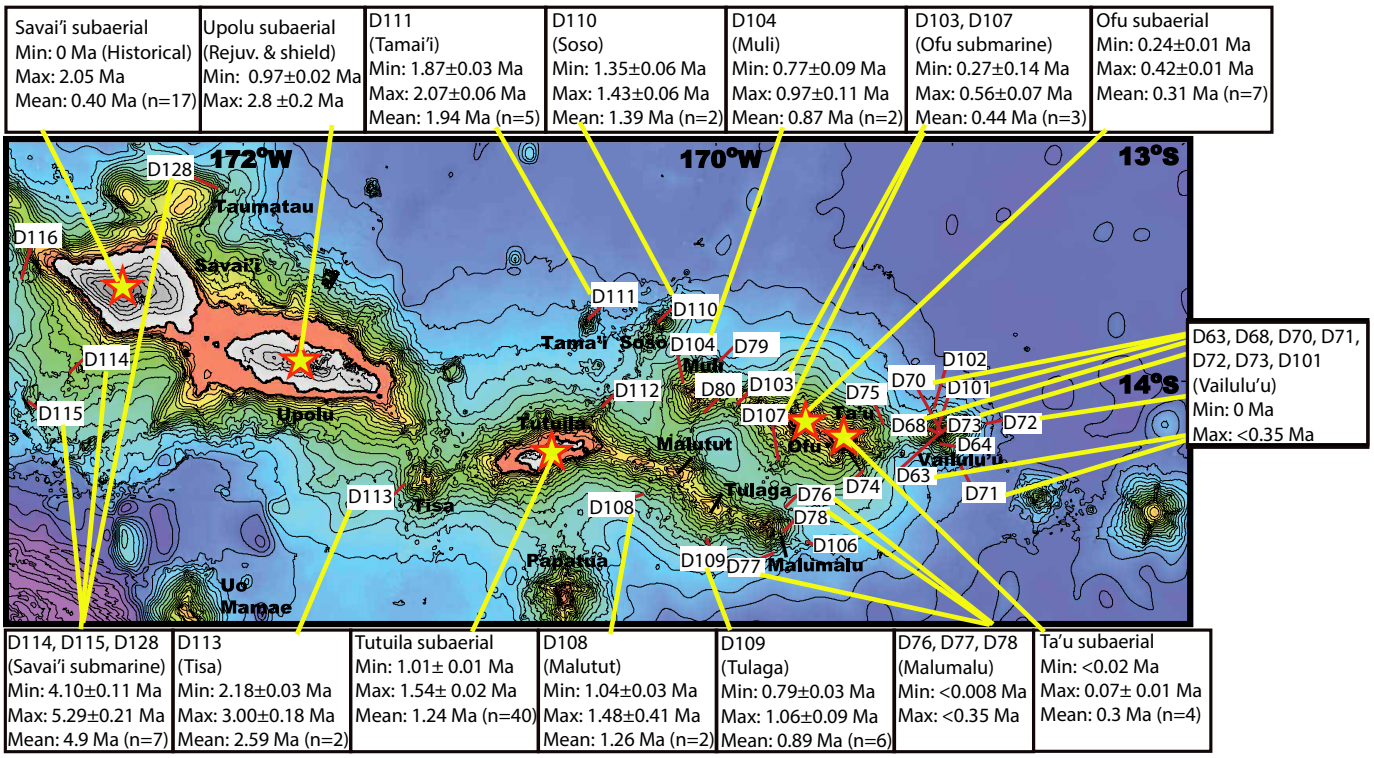

Extended Data Figure 1 | Sample locations and volcano ages. The range of ages for each location (subaerial or submarine dredge) is provided in a box at the periphery of the map, and a yellow line connects each location with the respective age data; not all samples with geochemical data have age data (indeed, most Samoan samples with geochemical data, submarine and subaerial, do not have age constraints). Dredge locations are labelled with a red line: dredges from the 1999 AVON2/3 cruise aboard the RV *Melville*[17] have dredge numbers less than 100, and dredges from the 2005 ALIA cruise aboard the RV *Kilo Moana*[18,19,39] have dredge numbers greater than 100. Samples collected on land were taken from the five Samoan islands (and are labelled with yellow stars: Savai'i subaerial, Upolu subaerial, Tutuila subaerial, Ta'u subaerial and Ofu subaerial). Malumalu and Vailulu'u seamount ages are based on uranium-series disequilibrium, and therefore maximum ages are provided[65,66]. Upolu subaerial lavas include both rejuvenated series (which bracket the younger limit of ages) and the shield series (which bracket the older limit of ages); poor outcrop exposure on the highly vegetated Samoan islands can make designation of the volcanic stages difficult (particularly if geochemical data are not available for the hand sample), and an average age for the rejuvenated or shield stages on Upolu is therefore not provided. Rejuvenated lavas are present on Tutuila, but ages are not available in the literature. All reported subaerial lavas from Savai'i are rejuvenated, indicating that the island has been covered with a veneer of rejuvenated volcanism[21,28]. Rejuvenated volcanism has been observed during historical times on Savai'i, which was last active from 1905–1911 (ref. 67); error bars are not provided for the oldest Savai'i subaerial sample in ref. 17. Submarine samples dredged off the coast of Savai'i (D114, D115 and D128) and from Tisa seamount were dredged distal to the Upo lineament and may not belong to this lineament. All available ages for Samoan islands and seamounts are provided in refs 17, 18, 39, 40, 41, 65, 66, 68 and 69. (Ma, million years.)

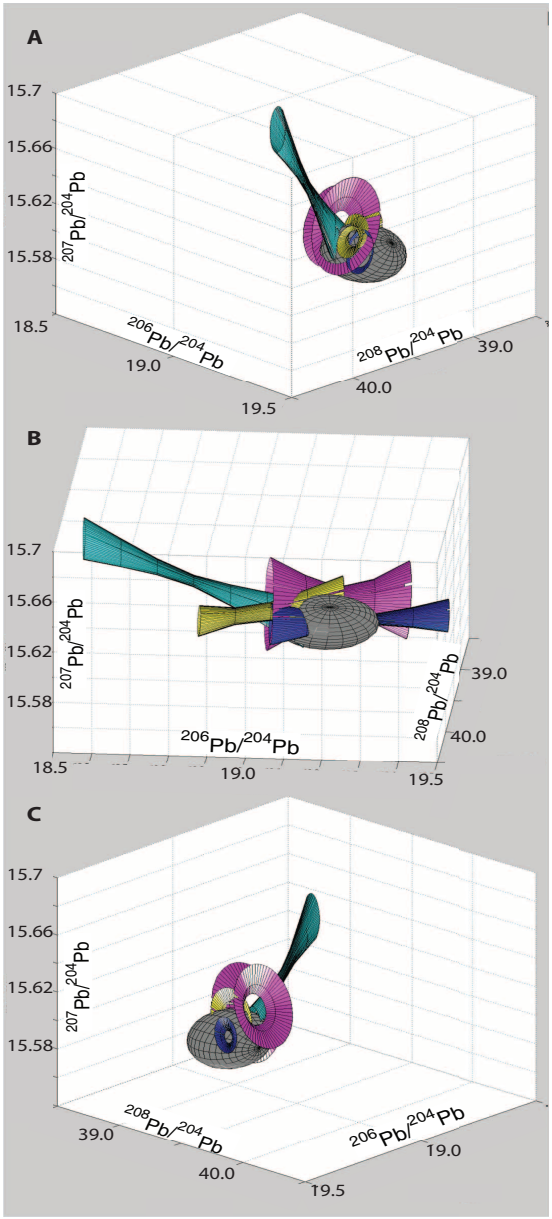

Extended Data Figure 2 | A three-dimensional presentation of the Pb-isotopic groups shows that they converge on the high $^3He/^4He$ common component region. 99% confidence intervals (appearing as 'tubes') around the best-fit lines through each of the four data groups—Malu lineament (pink tube), Vai lineament (dark blue), subaerial Upo lineament (yellow) and rejuvenated lavas (light blue)—are shown in three-dimensional Pb-isotopic space. The composition of the common component region is modelled as an ellipsoid (grey) that is defined by the 2σ variance around the average in the Pb-isotopic compositions for samples with $^3He/^4He > 20$ Ra. In three-dimensional Pb-isotopic space, the 99% confidence intervals around each of the best-fit trend lines overlap with the ellipsoid that encompasses the common component region. Each tube represents an estimate of the error around the best-fit trend to the data defining each geographic lineament. The tube therefore encloses the set of all possible mixing arrays associated with a given geographic lineament. Since all the tubes intersect the ellipsoid of the common component region, statistically a range of mixing arrays exists for each geographic lineament that passes through the common component region. This result is consistent with the compositional data of the four lineaments mixing with the high-$^3He/^4He$ common component.

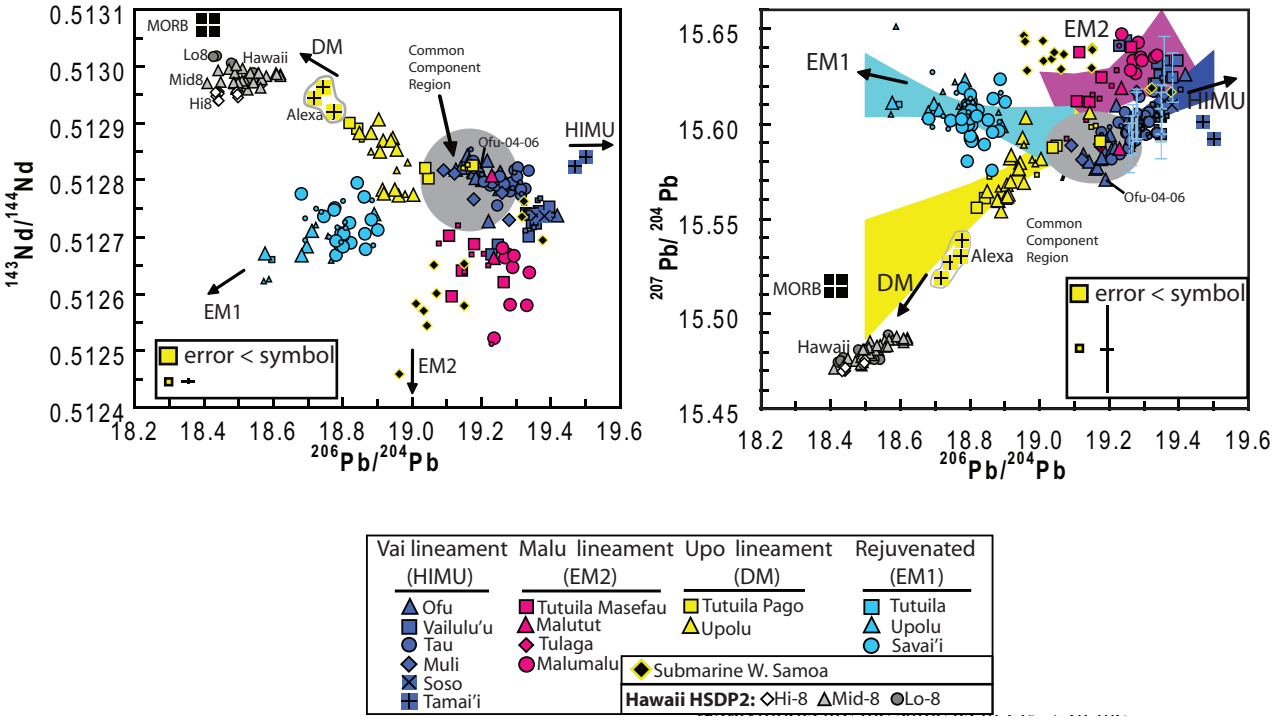

Extended Data Figure 3 | The isotopic composition of the four Samoan data groups are shown in Nd and Pb isotopic spaces. In both panels, the high-$^{3}He/^{4}He$ common component region is modelled by a grey ellipse that defines the 2σ variance around the average of the heavy radiogenic isotopic compositions of Samoan lavas with $^{3}He/^{4}He > 20$ Ra. The left panel shows the four data groups identified in Pb-isotopic space (Fig. 2) in a plot of $^{143}Nd/^{144}Nd$ versus $^{206}Pb/^{204}Pb$. Samples for which Pb-isotopic ratios were measured by high-precision techniques (Pb-spiked samples run by TIMS and samples run using Tl-addition by MC-ICP-MS) are shown as large symbols (where estimated 2σ external uncertainties are smaller than the symbols[17,19–21,29,38]), and unspiked Pb-isotopic TIMS data are shown as small symbols (where estimated 2σ external uncertainties are equal to or better than $\pm$0.076 for the $^{208}Pb/^{204}Pb$ ratio, as shown[14,17,48,51]). The right panel shows the four data groups identified in Fig. 2 in a plot of $^{206}Pb/^{204}Pb$ versus $^{207}Pb/^{204}Pb$. Samples for which Pb-isotopic ratios were measured by high-precision techniques (Pb-spiked samples run by TIMS and samples run using Tl-addition by MC-ICP-MS) are shown as large symbols (where estimated 2σ external uncertainties are smaller than the symbols, except for samples run on the P54 at Carnegie, where estimated 2σ external precision error bars are shown on the individual data points, as reported in the Methods); unspiked Pb-isotopic TIMS data are shown as small symbols (where estimated 2σ external uncertainties are equal to or better than $\pm$0.019 and $\pm$0.023 for $^{206}Pb/^{204}Pb$ and $^{207}Pb/^{204}Pb$, respectively, as shown). 99% confidence intervals around the best-fit lines through each data group overlap with the high-$^{3}He/^{4}He$ common component region. Symbols are the same as in Fig. 2 of the main text. The MORB average composition is from ref. 55. The HSDP-2 drill core data are from refs 24 and 30. See Supplementary Table 4 for a compilation of the Samoan data shown; Alexa data are from ref. 29.

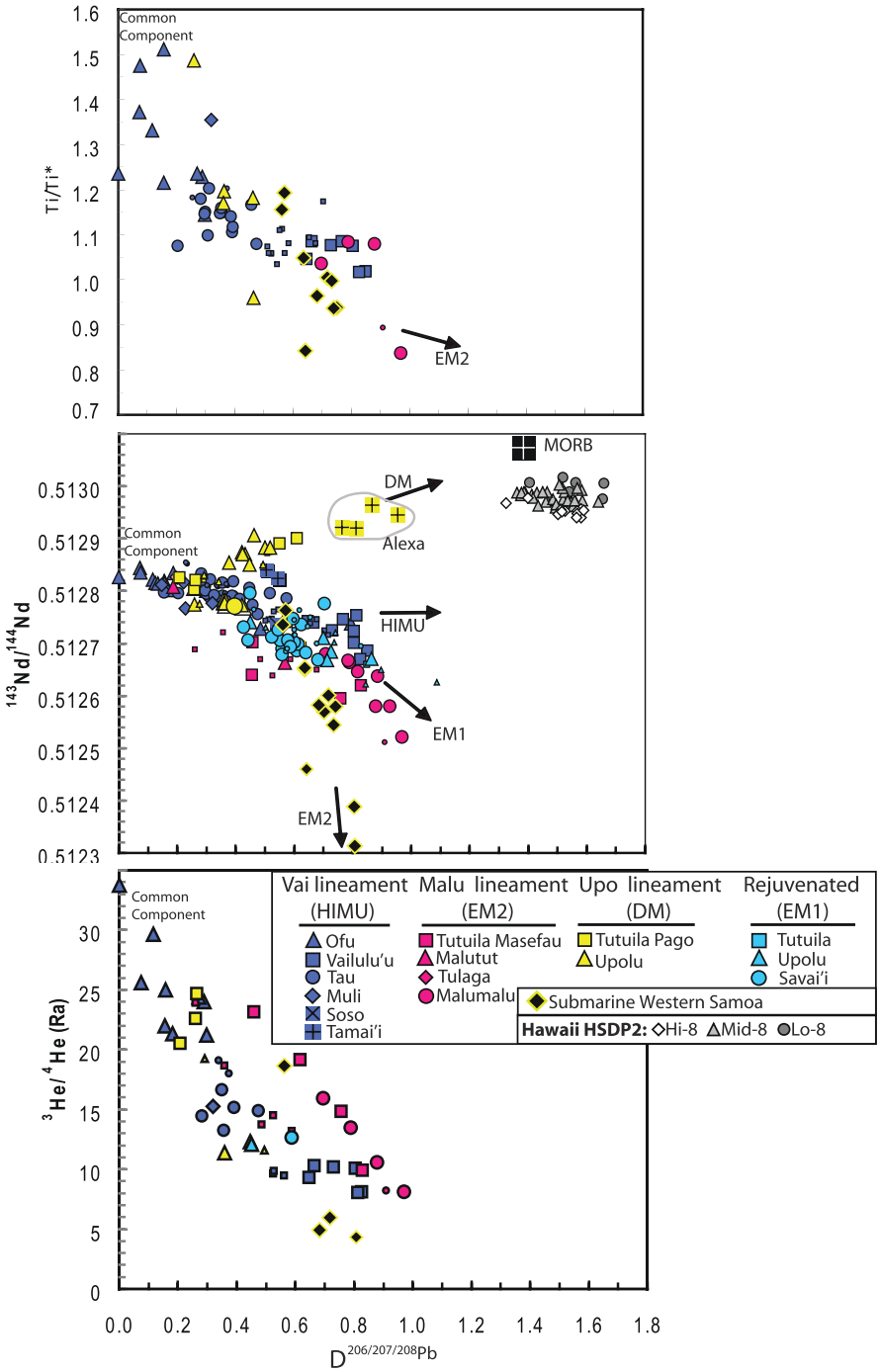

Extended Data Figure 4 | Various geochemical signatures show clear trends with increasing distance from the common component region in Pb-isotopic space. The top panel shows a plot of $D^{206/207/208}$Pb versus Ti/Ti*. Samoan lavas with the highest ^{3}He/^{4}He have the highest Ti/Ti* and the lowest $D^{206/207/208}$Pb values; this follows from an earlier observation that Ti/Ti* correlates with ^{3}He/^{4}He in Samoan lavas, and the high-^{3}He/^{4}He mantle reservoir has elevated Ti/Ti* (ref. 60). Ti/Ti* is defined in ref. 19. Only lavas with MgO > 7 wt% are shown, to avoid the effects of fractional crystallization of trace phases that might fractionate the trace element ratios. A sample with high MnO from Soso (ALIA110-39) is excluded owing to a high degree of alteration. ALIA-115-07, which is highly altered, is also excluded, as are all samples from ALIA Dredge 118. Samples with He concentrations $<10^{-9}$ cm^{3} of ^{4}He at STP per gram of sample (olivine) are excluded. Additionally, only shield-stage lavas are plotted. The middle panel shows $D^{206/207/208}$Pb versus ^{143}Nd/^{144}Nd. ^{143}Nd/^{144}Nd shows systematic behaviour in each data group moving away from the common component region (that is, with increasing $D^{206/207/208}$Pb) in Pb-isotope space. Data from subaerial Upo-lineament lavas (yellow) exhibit increasing ^{143}Nd/^{144}Nd with increasing distance (higher $D^{206/207/208}$Pb) from the common component region, and this supports the hypothesis that the subaerial portion of the Upo lineament samples a depleted mantle (DM) component similar to that found in the Alexa seamount and Hawaii. The other data groups (from the rejuvenated lavas and the Vai and Malu volcanic lineaments) all exhibit lower (more enriched) ^{143}Nd/^{144}Nd with increasing distance from the common component region. Finally, the middle panel shows that ^{143}Nd/^{144}Nd exhibits the least amount of variability in the common component region—where $D^{206/207/208}$Pb is zero—as the four isotopic groups converge on a common component with relatively homogeneous isotopic characteristics. The bottom panel shows $D^{206/207/208}$Pb versus ^{3}He/^{4}He (also shown in Fig. 2 of the main text) for comparison with the other panels. Symbols are the same as in Fig. 2. The MORB average composition is from ref. 55. The HSDP-2 drill core data are from refs 24 and 30. When calculating Ti/Ti*, only data obtained by ICP-MS (except Ti, which is measured by X-ray fluorescence) are used. See Supplementary Table 4 for sources of the Samoan data; Alexa data are from ref. 29.

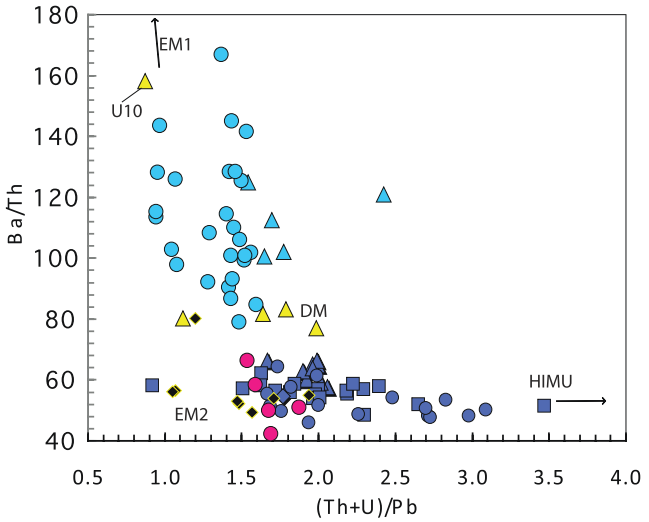

Extended Data Figure 5 | (U+Th)/Pb versus Ba/Th. Vai-lineament lavas exhibit the highest (U+Th)/Pb values in Samoa, consistent with a HIMU signature. Such high (U+Th)/Pb values are consistent with the radiogenic Pb-isotopic compositions in Vai-lineament lavas and similar to the high (U+Th)/Pb values observed in HIMU lavas. Samoan rejuvenated lavas, which have an EM1 signature, have high Ba/Th (and Ba/Sm and Ba/Nb); this Ba-enrichment matches the positive Ba-anomalies observed in EM1 endmember lavas from Pitcairn[29]. Highly altered samples and samples with low MgO are excluded (as described in Extended Data Fig. 4). Ref. 17 identified Upolu sample U10 as an outlier in many isotope and trace element spaces. Symbols are the same as in Fig. 2 of the main text. Only data obtained by ICP-MS are shown. See Supplementary Table 4 for a compilation of the Samoan data shown.

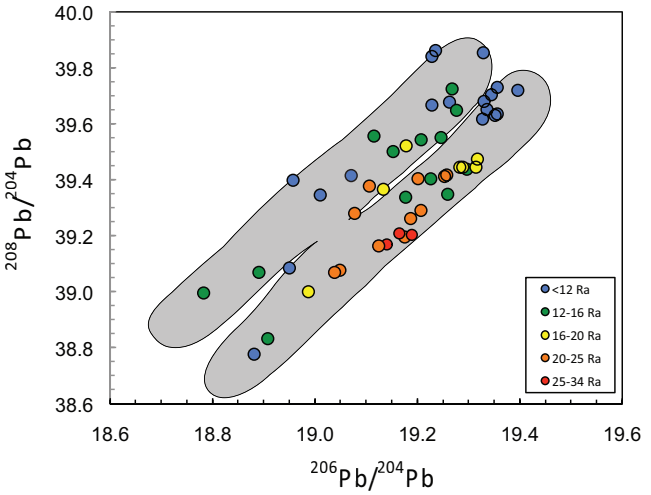

Extended Data Figure 6 | The $^{3}He/^{4}He$ ratios of Samoan lavas are shown in colour (warmer colours represent higher $^{3}He/^{4}He$) to show the distribution of $^{3}He/^{4}He$ ratios in $^{208}Pb/^{204}Pb$ versus $^{206}Pb/^{204}Pb$ isotopic space. Lavas with the highest $^{3}He/^{4}He$ tend to cluster near the region in Pb-isotopic space where the four Pb-isotopic data groups converge, and lavas with lower $^{3}He/^{4}He$ tend to plot farthest from the common component region. Samples with $<10^{-9}$ cm^{3} of ^{4}He at STP per gram of sample (olivine) are excluded. See Supplementary Table 4 for a compilation of the Samoan data shown.